View metadata, citation and similar papers at core.ac.uk

brought to you by CORE

provided by Queen Mary Research Online

Nanoscale

Accepted Manuscript

This article can be cited before page numbers have been issued, to do this please use: X. ZHAO, T. Liu, W. SHI, X. HOU and T. J.S. Dennis, *Nanoscale*, 2019, DOI: 10.1039/C8NR08890J.

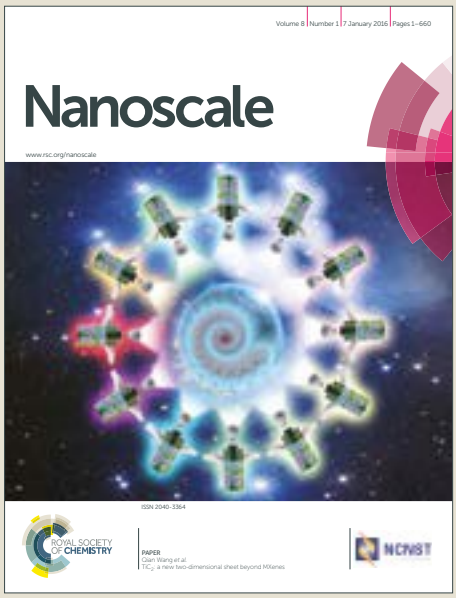

This is an Accepted Manuscript, which has been through the Royal Society of Chemistry peer review process and has been accepted for publication.

Accepted Manuscripts are published online shortly after acceptance, before technical editing, formatting and proof reading. Using this free service, authors can make their results available to the community, in citable form, before we publish the edited article. We will replace this Accepted Manuscript with the edited and formatted Advance Article as soon as it is available.

You can find more information about Accepted Manuscripts in the author guidelines.

Please note that technical editing may introduce minor changes to the text and/or graphics, which may alter content. The journal's standard Terms & Conditions and the ethical guidelines, outlined in our author and reviewer resource centre, still apply. In no event shall the Royal Society of Chemistry be held responsible for any errors or omissions in this Accepted Manuscript or any consequences arising from the use of any information it contains.

View Article Online
DOI: 10.1039/C8NR08890J

Published on 08 January 2019. Downloaded by Queen Mary, University of London on 1/13/2019 5:07:49 PM.

Capillary-Written Single-Crystalline All-Inorganic Perovskite Microribbon Arrays for Highly-Sensitive and Thermal-Stable Photodetectors

Xiaoming Zhao,[1,#,*] Tianjun Liu,[2] Wenda Shi,[1] Xueyan Hou[1] and T. John S. Dennis[1*]

[1] School of Physics and Astronomy, Queen Mary University of London, Mile End Road, London E1 4NS, United Kingdom

[2] School of Engineering and Materials Science, Queen Mary University of London, Mile End Road, London E1 4NS, United Kingdom.

[#] Present Address: Department of Chemical and Biological Engineering, Princeton University, Princeton, New Jersey 08544, United States

*Email: Xiaoming Zhao (email: xiaoming.zhao@qmul.ac.uk), T. John S. Dennis (email: j.dennis@qmul.ac.uk)

KEYWORDS: single crystals; all-inorganic perovskite; microribbon; photodetector.

ABSTRACT: In recent times, as a result of its exceptional resistance to moisture and heat, cesium lead bromide ($CsPbBr_3$) was established as a potential high-performance perovskite material for optoelectronics, which is inclusive of photodetectors and photovoltaics. It has been demonstrated that perovskite single crystal has major benefits over its thin-film equivalents; nevertheless, the preparation of perovskite crystal arrays for the utilisation of extensive integration is a challenging task. In this paper, we consider a simple crystallisation system, being a capillary-written system to enable the growth of single crystal microribbon arrays (MRAs) directly from a precursor solution.

Nanoscale Accepted Manuscript

View Article Online
DOI: 10.1039/C8NR08890J

Published on 08 January 2019. Downloaded by Queen Mary, University of London on 1/13/2019 5:07:49 PM.

It is demonstrated by microstructure characterisation that $CsPbBr_3$ MRAs are good-quality single crystals with highly-aligned crystal packing and smooth surfaces. The band-edge photoluminescence (PL) is exceptionally resilient and has a lengthy PL life of ~62 ns. An exceptional photo-response having a particularly 99 μs quick response time and a 2496 A W^{-1} ultra-high responsivity is exhibited by photodetectors which are built upon these MRAs. The fact that as-fabricated photodetectors maintain 90% of their commencing performance following 100 days of constant stress testing in ambient conditions under an illumination of 450 nm, showing exceptional operational stability, is noteworthy. A significant step towards the large-area growth of high-quality perovskite MRAs is presented by this work. This supplies favourable opportunities to build high-performance optoelectronic and nanophotonic systems.

In recent times, as a result of their exceptional optoelectronic attributes, hybrid organic-inorganic lead halide perovskites have displayed considerable potential applications in photodetectors (PDs), lasers and light-emitting diodes and also particularly in solar cells.[1–7] Single crystals, as well as polycrystalline films are utilised in order to construct perovskite photodetectors.[8–11] Benefits greater than those of polycrystalline are shown by the optoelectronic attributes of single crystals which are connected with lifetimes, carrier mobilities and single crystals' defect tolerance.[12–16] These draw global awareness on single-crystal photodetectors which were perovskite-based.[17–20] The usage of hybrid lead halide perovskites as long-term devices under light, heat or moisture is seriously restricted by their instabilities.[21] Several different

Nanoscale Accepted Manuscript

View Article Online
DOI: 10.1039/C8NR08890J

Published on 08 January 2019. Downloaded by Queen Mary, University of London on 1/13/2019 5:07:49 PM.

strategies are suggested to address this instability such as additive engineering, crystal engineering, interface engineering and composition engineering, and most encouraging one is the replacement of organic compounds with inorganic ones.[22–28] Noteworthy attributes are displayed by all-inorganic perovskite $CsPbBr_3$. These include narrow emission line width, direct optical band gap, high luminescence, high quantum yields and large optical absorption across the visible spectra band.[29,30] Massive possible applications in the areas of photodetection, solar cells, lasers and LEDs are enabled by these attributes.[31–34] Despite the fact that solution-based systems have realised several $CsPbBr_3$ nanostructures; for example, nanowires, nanoplates and quantum dots, there are few system which has the capacity to attain large-area scale growth of highly-ordered $CsPbBr_3$ nanostructure arrays together with horizontal alignment upon surfaces, which is particularly advantageous in future integrated devices, is reported.[35–41]

In this paper, the application of a capillary-written system achieves a successful crystal growth of highly-aligned $CsPbBr_3$ perovskite microribbon arrays is reported. The excellent quality single-crystalline attributes of the achieved microribbons are portrayed by the microstructure characterisations. This was presented to a greater extent by the strong band-edge photoluminescence having a long PL lifetime. A responsivity of 2496 A W^{-1} and a particularly rapid response of 99 μs were attained by high-performance photodetectors on the basis of as-prepared MRAs (**Table 1**).[42–52] It is worthy of mention that following 100 days of constant stress testing in ambient conditions under an illumination of 450nm, as-prepared photodetectors remain 90% of

Nanoscale Accepted Manuscript

View Article Online
DOI: 10.1039/C8NR08890J

their starting performance, which clearly shows its high-quality operational stability. A significant step towards preparation of well-aligned perovskite nanostructures is attained by this study with regard to usage in on-chip integrated photonics systems and high-density optoelectronic devices.

A representational diagram of a directly written system which applies a hollow rectangular capillary for the purpose of attaining $CsPbBr_3$ MRAs is depicted in **Figure 1a**. Capillary forces hold a precursor solution with an equimolar ratio of $CsBr:PbBr_2$ (1:1) within dimethyl sulfoxide (DMSO) in the capillary. As a result of its general greater solubility restriction for the precursors, we chose DMSO as a solvent rather than N,N-dimethylformamide (DMF). In order to mould an "L" shape, the capillary is bent at 1cm to enable the maintenance of a gravity feed at consistent pressure, which relates to the height of the vertical part. A computer-controlled linear translation stage is used to mount a substrate. This stage includes a thermoelectric module to achieve temperature control. We achieve film deposition by permitting a solution microdroplet to the end of the capillary in order to make contact with the surface and subsequently to translate the substrate at a controlled rate of 0.02 mm s^{-1}. Following the evaporation of the solvent on the hotplate for 15 minutes at 80 °C, it is annealed for further three minutes at 120 °C. This results in the formation of highly-aligned single-crystal microribbon arrays as depicted in atomic force microscope (AFM) images in **Figure 1b**. Nanoscale AFM (**Figure S1**) indicates the uniform morphology of individual micro-ribbon. The average width of (58 ± 9) nm and thickness of (5.6 ± 0.8) μm is obtained based on the examination of 50 individual micro-ribbons.

Published on 08 January 2019. Downloaded by Queen Mary, University of London on 1/13/2019 5:07:49 PM.

Nanoscale Accepted Manuscript

View Article Online
DOI: 10.1039/C8NR08890J

Published on 08 January 2019. Downloaded by Queen Mary, University of London on 1/13/2019 5:07:49 PM.

As shown in **Figure 1c** and **d**, the rotated crystals extinguish simultaneously as single crystals between crossed polarizers, which is the supporting evidence for the single-crystallinity nature and long-range ordering of as-prepared MRAs. High-magnification scanning electron microscope (SEM) images (**Figures 1e**) of one individual micro-ribbon further demonstrate the ultrasmooth surface of as-grown MRs, with well-defined crystal edge.

In order to be certain that the MRAs' crystal structure conformed to the anticipated room-temperature orthorhombic phase $CsPbBr_3$, the said structure was quantified. Strong diffraction peaks are depicted by the $CsPbBr_3$ X-ray diffraction (XRD) pattern. All diffraction peaks can be indexed to orthorhombic phase $CsPbBr_3$, and no other impurity peaks were observed. (**Figure 1f**). There is additional indication by the distinct splitting of the narrow 101 and 020 peaks that the as-grown $CsPbBr_3$ comprises the room-temperature orthorhombic phase. We obtain additional awareness of the crystal structure through the transmission electron microscope (TEM) of separate crystal together with its relative selected area electron diffraction (SAED) patterns (**Figure 1g**). The fact that the micro-ribbons are single crystalline is verified by the SAED pattern as depicted in **Figure 1g (inset)**. Diffraction spots corresponding to the zone axes of [202] and [002] of orthorhombic phase $CsPbBr_3$ were indexed in the SAED pattern. Therefore, based on the analysis of the AFM images, polarized optical images, SEM images, the XRD pattern, and the TEM-SAED pattern, we conclude that single-crystalline $CsPbBr_3$ microribbon arrays have been obtained.

Nanoscale Accepted Manuscript

View Article Online
DOI: 10.1039/C8NR08890J

Published on 08 January 2019. Downloaded by Queen Mary, University of London on 1/13/2019 5:07:49 PM.

The photoluminescence spectra and optical absorption of $CsPbBr_3$ single crystal MRAs are shown in **Figure 2a**. With the position of the absorption edge being 559nm, we calculated the energy band gap (E_g) to be 2.19 eV, less than its thin-film equivalent, whose energy band gap is 2.32 eV.[53] It is implied by the lower E_g value that single crystal is more appropriate than polycrystalline film when it is used as a photodetector. We identified the PL peak centred at 558 nm from the PL spectrum having an excitation of 443 nm. Furthermore, it was implied that the near-edge defect levels were associated with the surface states which occupied a function in the emission procedure since the PL emission width ranged from 510 to 590 nm.[54] A biexponential profile was fitted to the PL decay curve, which indicated a long PL lifetime of $\tau_1 = 6.9$ and $\tau_2 = 62.4$ ns as depicted in **Figure 2b**. The high-quality optical abilities of the highly-aligned perovskite MRAs are shown by the aforementioned optical attributes which are of assistance in realising high-performance optoelectronic devices.

The photodetector devices were fabricated on the basis of MRAs having gold (50 nm) as source and drain electrodes in order to examine the photoelectronic attributes of the $CsPbBr_3$ MRAs. **Figure 3a** illustrates the representational diagram of the as-fabricated device. It is depicted in **Figure 3b** that we measured the current-voltage (*I-V*) curves of the device in darkness and under 450 nm illumination of various power intensities. The photocurrent is proportional to the illumination intensity and the drain voltage. We calculated photoresponsivity (R) and gain (G), which are significant photodetector parameters by using equations (1) and (2), [51,55–57]

$$R = \frac{I_{light} - I_{dark}}{PS} \quad (1)$$

Nanoscale Accepted Manuscript

View Article Online
DOI: 10.1039/C8NR08890J

$$G = \frac{I_{light} - I_{dark} / e}{PS / hv} \quad (2)$$

where I_{light} is the current under illumination, I_{dark} is the dark current, P is the incident power density and S is the effective area, hv is the energy of an incident photon and e is electronic charge. The gain of the device and its illumination power-dependent responsivity are depicted in **Figure 3c** which shows a high gain of 6.9×10^3 and a high responsivity of 2.5×10^3 A W^{-1} at a bias voltage of 3 V under just 0.01 mW cm^{-2} illumination. This indicates the photodetectors' high sensitivity. As shown in **Figure 3d**, the gain and responsivity are plotted as a function of the bias. The important improvement in the performance by increasing the drain voltage is demonstrated by the detector. Furthermore, **Figure S2** in the supporting information, depicts the wavelength-dependent responsivity, thereby showing the broadband high photo-response ranging from UV to the visible area.

With regard to a photodetector's optoelectronic applications, a rapid response to optical signals is crucial. The time-dependent response of photodetectors, where the laser is on and off at a 3V fixed voltage, is depicted in **Figure 3e**. The "on" and "off" states keep the identical current level for many cycles under the illumination of the identical power density. This shows the exceptional stability and reversibility of $CsPbBr_3$ MRA photodetectors. Moreover, it is shown by analysis of a photo-response process comprising of both reset and rising process that both times are close to 100 μs (**Figure 3f**). As depicted in **Table 1**, all of these values are among highest for all-inorganic perovskite PDs.[42–52]

Published on 08 January 2019. Downloaded by Queen Mary, University of London on 1/13/2019 5:07:49 PM.

Nanoscale Accepted Manuscript

View Article Online
DOI: 10.1039/C8NR08890J

Published on 08 January 2019. Downloaded by Queen Mary, University of London on 1/13/2019 5:07:49 PM.

In our study, the perovskite microribbon devices not only showed good performances but also an exceptionally high stability as a result of their all-inorganic composition. **Figure 4a** indicates that when the PDs were stored in a high-temperature environment (80 ℃, 40% ~ 50% R.H.) or under nitrogen atmosphere, there was no evident performance degeneration. Furthermore, it is worthy of mention that, under constant illumination of 450nm, the PDs offer good-quality stability and, after 1000 hours, maintain over 95% of their initial performance. Moreover, **Figure 4b** demonstrated the negligible reduction of the photocurrent following constant illumination of 450 nm for a period of 100 days. This further shows our device's good stability.

To summarise, we applied a capillary-written system which led to a successful preparation of highly-aligned $CsPbBr_3$ perovskite microribbon arrays. We demonstrated as-grown MRAs as excellent quality single crystals which have well-adjusted crystal packing as well as smooth surfaces. The photodetectors which are built upon these MRAs show an exceptional photo response at a very rapid response of 99 μs and an ultra-high responsivity of 2496 A W^{-1}. It is worthy of mention that as-fabricated photodetectors, after 100 days of constant stress testing, keep more than 90% of the starting performance when tested under ambient conditions under 450 nm illumination. This offers exceptional operational stability, which shows a novel practical advantage for a greatly aligned perovskite nanostructures. In this system, we can advance significant application in optoelectronic systems and chip-scale integrated photonics.

Nanoscale Accepted Manuscript

View Article Online
DOI: 10.1039/C8NR08890J

Published on 08 January 2019. Downloaded by Queen Mary, University of London on 1/13/2019 5:07:49 PM.

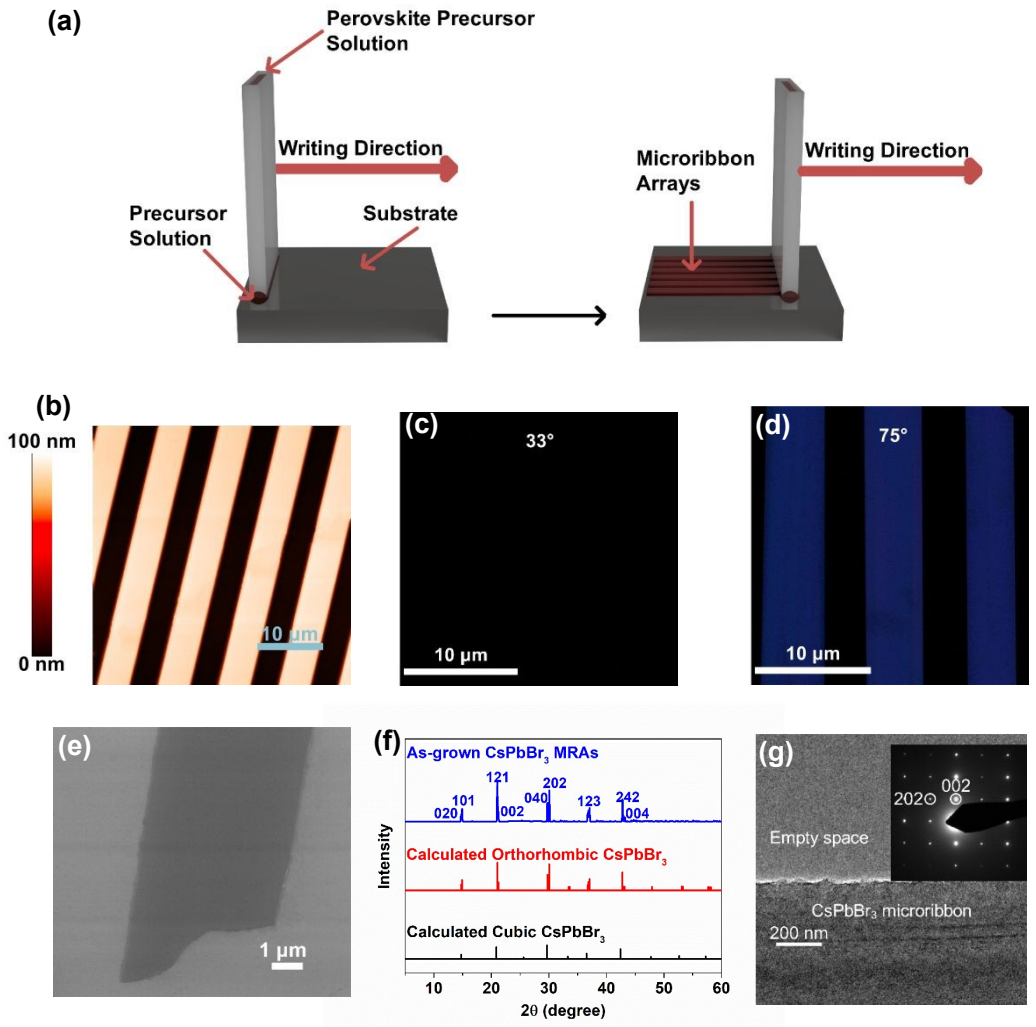

Figure 1 (a) A representational diagram of the preparation of $CsPbBr_3$ single-crystalline microribbon arrays by means of a hollow capillary writing system; (b) An AFM image of $CsPbBr_3$ single-crystalline MRAs; Optical images of $CsPbBr_3$ single-crystalline MRAs under crossed polarizers of (c) 33° and (d) 75°, respectively; (e) An SEM image of individual $CsPbBr_3$ microribbon; (f) An XRD pattern of as-grown $CsPbBr_3$ single crystals as well as the XRD patterns of orthorhombic and cubic $CsPbBr_3$; (g) TEM image and (inset) associate electron diffraction pattern of a $CsPbBr_3$ single-crystalline microribbon.

Nanoscale Accepted Manuscript

View Article Online
DOI: 10.1039/C8NR08890J

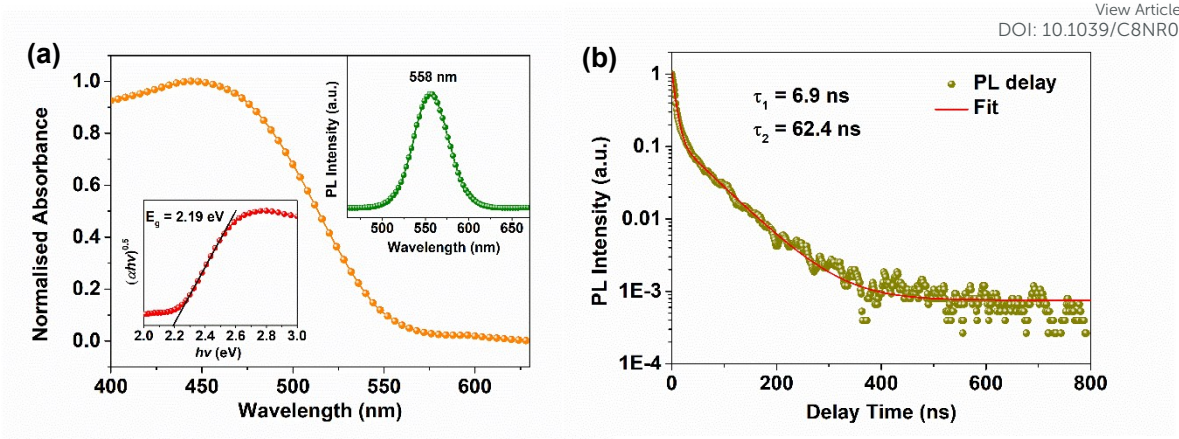

Figure 2 (a) Absorption atrributes of the $CsPbBr_3$ microribbonarrays. Insets show the Tauc plot (lower inset) and the steady-state PL data (upper inset); (b) Time-resolved PL (λ_{exc} = 443 nm) spectrum of $CsPbBr_3$ microribbon arrays.

Published on 08 January 2019. Downloaded by Queen Mary, University of London on 1/13/2019 5:07:49 PM.

Nanoscale Accepted Manuscript

View Article Online
DOI: 10.1039/C8NR08890J

Published on 08 January 2019. Downloaded by Queen Mary, University of London on 1/13/2019 5:07:49 PM.

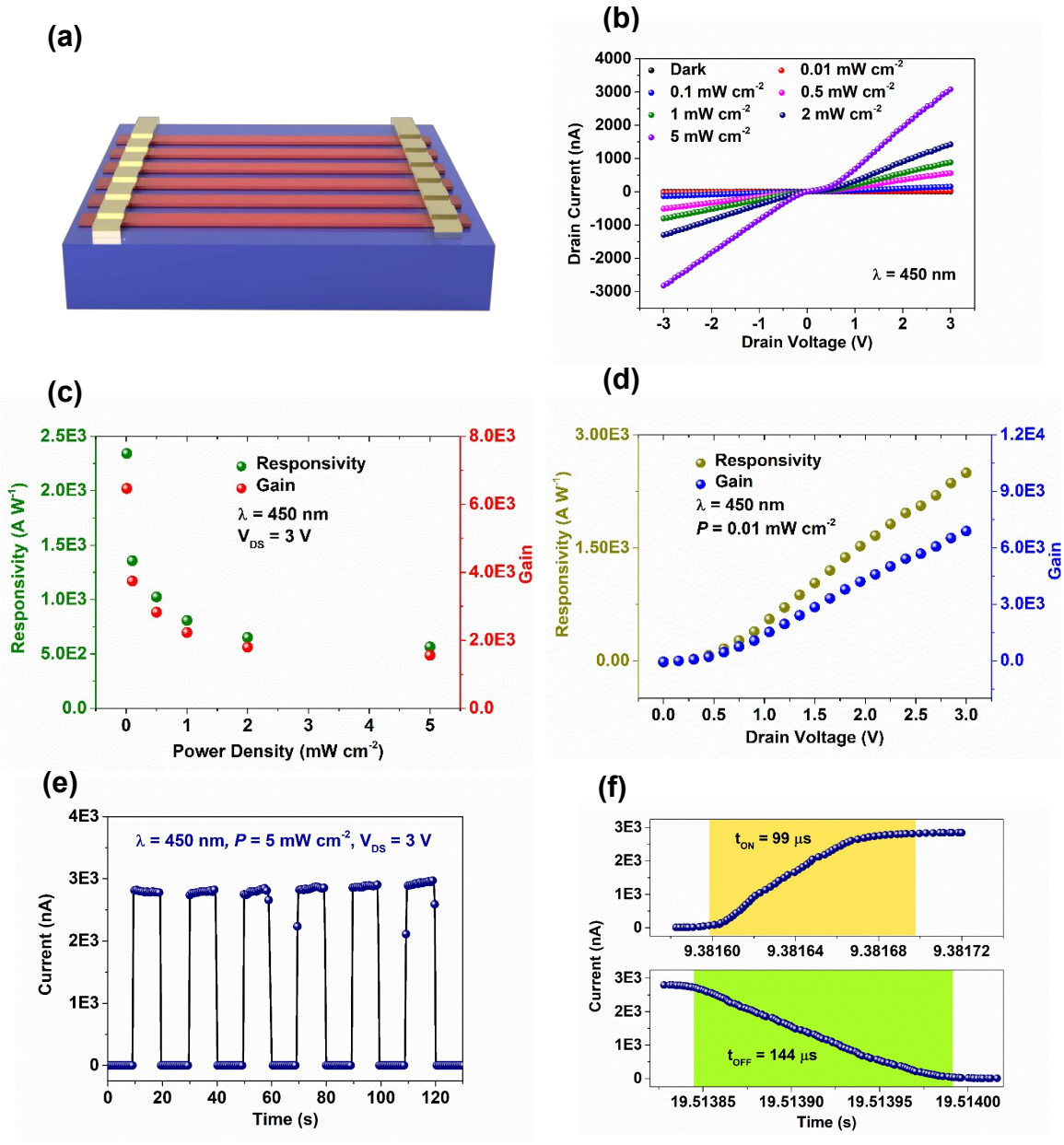

Figure 3 (a) A representational diagram of the as-fabricated device; (b) *I-V* curves of the device in darkness and below 450 nm illumination of various intensities; (c) Responsivity and gain *vs* light intensity plotted at a 3 V bias; (d) Gain and responsivity as a function of the bias voltage (irradiance 0.01 mW cm^{-2}); (e) Time-resolved response of the device in darkness and in light illumination; (f) Photodetector ON and OFF times.

Nanoscale Accepted Manuscript

View Article Online
DOI: 10.1039/C8NR08890J

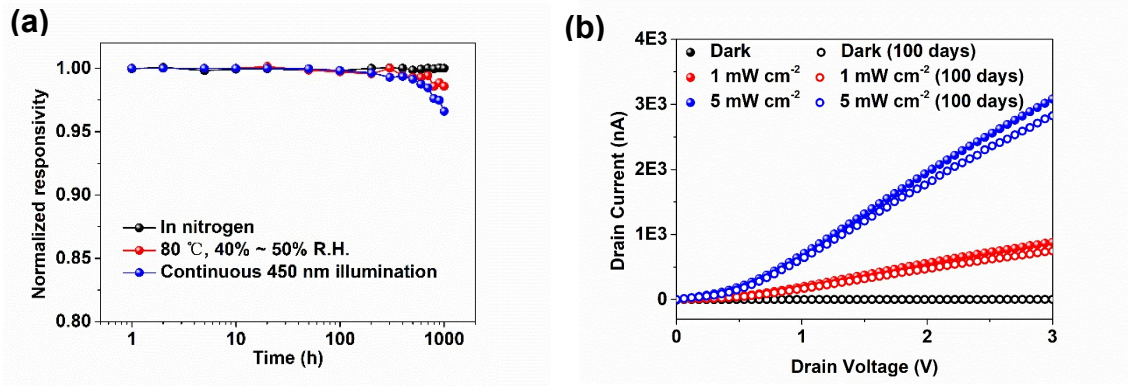

Figure 4 (a) Time course of the change of the normalised responsivity of as-prepared photodetectors under various storage conditions. (b) *I-V* attributes of as-prepared photodetectors under various irradiance prior to and subsequent to 100 days' light soaking under constant 450 nm illumination.

Published on 08 January 2019. Downloaded by Queen Mary, University of London on 1/13/2019 5:07:49 PM.

Nanoscale Accepted Manuscript

View Article Online
DOI: 10.1039/C8NR08890J

Table 1 Comparison of the device performance of all-inorganic perovskite PDs reported.

Photodetector	R [A W^{-1}]	t_{ON} [ms]	t_{OFF} [ms]	Stability	Ref.
$CsPbBr_3$ microparticles	0.18	1.8	1.0	> 2 month	[42]
$CsPbBr_3$ nanosheets	0.25	0.019	0.025	> 12 h	[43]
$CsPbBr_3$ thin films	55	0.43	0.32		[44]
$CsPbBr_3$ nanowires	1×10^3	0.02	0.02		[45]
$CsPbI_3$ nanowires	0.0067	292	234		[46]
$CsPbBr_3$ nanosheets	31.1	0.016	0.38		[47]
$CsPbBr_3$ nanoplatelets	34	0.6	0.9		[48]
$CsPbBr_3$ bulk crystals	0.028	0.23	0.06		[49]
$CsPbBr_3$ microcrystals	6×10^4	0.5	1.6		[50]
$CsPbBr_3$ nanowires	4.4×10^3	0.252	0.3		[51]
$CsPbI_3$ nanorods	2.92×10^3	0.05	0.15	> 1 week	[52]
$CsPbBr_3$ microribbon	2.496×10^3	0.099	0.144	> 100 days	Present Work

Published on 08 January 2019. Downloaded by Queen Mary, University of London on 1/13/2019 5:07:49 PM.

Nanoscale Accepted Manuscript

View Article Online
DOI: 10.1039/C8NR08890J

Published on 08 January 2019. Downloaded by Queen Mary, University of London on 1/13/2019 5:07:49 PM.

ASSOCIATED CONTENT

Supporting Information.

Experimental Section; Nanoscale AFM image and associated height analysis of $CsPbBr_3$ microribbon; Wavelength-dependent photo-responsivity.

AUTHOR INFORMATION

Corresponding Author

*Email: Xiaoming Zhao (email: xiaoming.zhao@qmul.ac.uk), T. John S. Dennis (email: j.dennis@qmul.ac.uk)

Notes

The authors declare no competing financial interest.

ACKNOWLEDGMENT

X. Zhao, T. Liu, X. Hou and W. Shi thank the China Scholarship Council for funding.

Nanoscale Accepted Manuscript

View Article Online
DOI: 10.1039/C8NR08890J

Published on 08 January 2019. Downloaded by Queen Mary, University of London on 1/13/2019 5:07:49 PM.

Nanoscale Accepted Manuscript

REFERENCES

1 H. Zhu, Y. Fu, F. Meng, X. Wu, Z. Gong, Q. Ding, M. V. Gustafsson, M. T. Trinh, S. Jin and X. Y. Zhu, *Nat. Mater.*, 2015, **14**, 636–642.

2 Y. Ling, Z. Yuan, Y. Tian, X. Wang, J. C. Wang, Y. Xin, K. Hanson, B. Ma and H. Gao, *Adv. Mater.*, 2016, **28**, 305–311.

3 Y. Lee, J. Kwon, E. Hwang, C. H. Ra, W. J. Yoo, J. H. Ahn, J. H. Park and J. H. Cho, *Adv. Mater.*, 2015, **27**, 41–46.

4 F. Zhang, W. Shi, J. Luo, N. Pellet, C. Yi, X. Li, X. Zhao, T. J. S. Dennis, X. Li, S. Wang, Y. Xiao, S. M. Zakeeruddin, D. Bi and M. Grätzel, *Adv. Mater.*, 2017, **29**, 1606806.

5 X. Zhao, F. Zhang, C. Yi, D. Bi, X. Bi, P. Wei, J. Luo, X. Liu, S. Wang, X. Li, S. M. Zakeeruddin and M. Grätzel, *J. Mater. Chem. A*, 2016, **4**, 16330–16334.

6 X. ZHAO, L. Tian, T. Liu, H. Liu, S. Wang, X. Li, O. Fenwick, S.-B. Lei and W. Hu, *J. Mater. Chem. A*, , DOI:10.1039/C8TA10510C.

7 F. Zhang, D. Bi, N. Pellet, C. Xiao, Z. Li, J. J. Berry, S. M. Zakeeruddin, K. Zhu and M. Grätzel, *Energy Environ. Sci.*, , DOI:10.1039/C8EE02252F.

8 D. Wu, H. Zhou, Z. Song, R. Liu and H. Wang, *J. Mater. Chem. C*, 2018, **6**, 8628–8637.

9 Z. Sun, L. Aigouy and Z. Chen, *Nanoscale*, 2016, **8**, 7377–7383.

View Article Online
DOI: 10.1039/C8NR08890J

10 G. Tong, H. Li, Z. Zhu, Y. Zhang, L. Yu, J. Xu and Y. Jiang, *J. Phys. Chem. Lett.*, 2018, **9**, 1592–1599.

11 J. Wang, F. Liu, G. Wang, L. Wang and C. Jiang, *Org. Electron.*, 2016, **38**, 158–163.

12 S. Du, L. Jing, X. Cheng, Y. Yuan, J. Ding, T. Zhou, X. Zhan and H. Cui, *J. Phys. Chem. Lett.*, 2018, **9**, 5833–5839.

13 X. Cheng, L. Jing, Y. Zhao, S. Du, J. Ding and T. Zhou, *J. Mater. Chem. C*, 2018, **6**, 1579–1586.

14 J. Ding, L. Jing, X. Cheng, Y. Zhao, S. Du, X. Zhan and H. Cui, *J. Phys. Chem. Lett.*, 2018, **9**, 216–221.

15 J. Ding, X. Cheng, L. Jing, T. Zhou, Y. Zhao and S. Du, *ACS Appl. Mater. Interfaces*, 2018, **10**, 845–850.

16 J. Ding, Y. Zhao, Y. Sun, S. Du, H. Cui, L. Jing, X. Cheng, Z. Zuo and X. Zhan, *Cryst. Res. Technol.*, 2017, **52**, 1700021.

17 X. Ren, Z. Yang, D. Yang, X. Zhang, D. Cui, Y. Liu, Q. Wei, H. Fan and S. F. Liu, *Nanoscale*, 2016, **8**, 3816–3822.

18 G. E. Eperon and D. S. Ginger, *Nat. Energy*, 2016, **1**, 16109.

19 X. Zhao, T. Liu, X. Hou, Z. Liu, W. Shi and T. J. S. Dennis, *J. Mater. Chem. C*, 2018, **6**, 5489–5496.

Published on 08 January 2019. Downloaded by Queen Mary, University of London on 1/13/2019 5:07:49 PM.

Nanoscale Accepted Manuscript

View Article Online
DOI: 10.1039/C8NR08890J

20 X. Zhao, T. Liu, Y. Zhang, S. Wang, X. Li, Y. Xiao, X. Hou, Z. Liu, W. Shi and T. J. S. Dennis, *Adv. Mater. Interfaces*, 2018, **5**, 1800336.

21 T. Leijtens, G. E. Eperon, N. K. Noel, S. N. Habisreutinger, A. Petrozza and H. J. Snaith, *Adv. Energy Mater.*, , DOI:10.1002/aenm.201500963.

22 W. Yongzhen, X. Fengxian, C. Han, Y. Xudong, S. Huimin, C. Molang, Z. Zhongmin, N. Takeshi and H. Liyuan, *Adv. Mater.*, 2017, **29**, 1701073.

23 T. Li, Y. Pan, Z. Wang, Y. Xia, Y. Chen and W. Huang, *J. Mater. Chem. A*, 2017, **5**, 12602–12652.

24 H. Zhou, Q. Chen, G. Li, S. Luo, T. -b. Song, H.-S. Duan, Z. Hong, J. You, Y. Liu and Y. Yang, *Science (80-.).*, 2014, **345**, 542–546.

25 X. Li, M. Ibrahim Dar, C. Yi, J. Luo, M. Tschumi, S. M. Zakeeruddin, M. K. Nazeeruddin, H. Han and M. Grätzel, *Nat. Chem.*, 2015, **7**, 703–711.

26 N. J. Jeon, J. H. Noh, W. S. Yang, Y. C. Kim, S. Ryu, J. Seo and S. Il Seok, *Nature*, 2015, **517**, 476–480.

27 J. Liang, C. Wang, Y. Wang, Z. Xu, Z. Lu, Y. Ma, H. Zhu, Y. Hu, C. Xiao, X. Yi, G. Zhu, H. Lv, L. Ma, T. Chen, Z. Tie, Z. Jin and J. Liu, *J. Am. Chem. Soc.*, 2016, **138**, 15829–15832.

28 S. R. J., E. G. E., M. Laura, P. E. S., K. B. A., P. J. B., H. M. T., J. M. B., H. A. Abbas, M. D. T. and S. H. J., *Adv. Energy Mater.*, 2016, **6**, 1502458.

Published on 08 January 2019. Downloaded by Queen Mary, University of London on 1/13/2019 5:07:49 PM.

Nanoscale Accepted Manuscript

View Article Online
DOI: 10.1039/C8NR08890J

Published on 08 January 2019. Downloaded by Queen Mary, University of London on 1/13/2019 5:07:49 PM.

29 R. F. Service, *Science (80-.).*, 2016, **351**, 113–114.

30 M. Kulbak, S. Gupta, N. Kedem, I. Levine, T. Bendikov, G. Hodes and D. Cahen, *J. Phys. Chem. Lett.*, 2016, **7**, 167–172.

31 L. Protesescu, S. Yakunin, M. I. Bodnarchuk, F. Krieg, R. Caputo, C. H. Hendon, R. X. Yang, A. Walsh and M. V. Kovalenko, *Nano Lett.*, 2015, **15**, 3692–3696.

32 S. W. Eaton, M. Lai, N. A. Gibson, A. B. Wong, L. Dou, J. Ma, L.-W. Wang, S. R. Leone and P. Yang, *Proc. Natl. Acad. Sci.*, 2016, **113**, 1993–1998.

33 X. Chang, W. Li, L. Zhu, H. Liu, H. Geng, S. Xiang, J. Liu and H. Chen, *ACS Appl. Mater. Interfaces*, 2016, **8**, 33649–33655.

34 J. Ding, S. Du, Z. Zuo, Y. Zhao, H. Cui and X. Zhan, *J. Phys. Chem. C*, 2017, **121**, 4917–4923.

35 Q. Zhang, R. Su, W. Du, X. Liu, L. Zhao, S. T. Ha and Q. Xiong, *Small Methods*, 2017, 1700163.

36 D. Zhang, Y. Yu, Y. Bekenstein, A. B. Wong, A. P. Alivisatos and P. Yang, *J. Am. Chem. Soc.*, 2016, **138**, 13155–13158.

37 D. Zhang, S. W. Eaton, Y. Yu, L. Dou and P. Yang, *J. Am. Chem. Soc.*, 2015, **137**, 9230–9233.

38 Y. Bekenstein, B. A. Koscher, S. W. Eaton, P. Yang and A. P. Alivisatos, *J. Am. Chem. Soc.*, 2015, **137**, 16008–16011.

Nanoscale Accepted Manuscript

View Article Online
DOI: 10.1039/C8NR08890J

39 Z. Liu, L. Jiao, Y. Yao, X. Xian and J. Zhang, *Adv. Mater.*, 2010, 22, 2285–2310.

40 Y. Zhang, X. Wang, Y. Wu, J. Jie, X. Zhang, Y. Xing, H. Wu, B. Zou, X. Zhang and X. Zhang, *J. Mater. Chem.*, 2012, **22**, 14357–14362.

41 J. Yao, H. Yan and C. M. Lieber, *Nat. Nanotechnol.*, 2013, **8**, 329–335.

42 X. Li, D. Yu, F. Cao, Y. Gu, Y. Wei, Y. Wu, J. Song and H. Zeng, *Adv. Funct. Mater.*, 2016, **26**, 5903–5912.

43 J. Song, L. Xu, J. Li, J. Xue, Y. Dong, X. Li and H. Zeng, *Adv. Mater.*, 2016, 4861–4869.

44 Y. Li, Z. F. Shi, S. Li, L. Z. Lei, H. F. Ji, D. Wu, T. T. Xu, Y. T. Tian and X. J. Li, *J. Mater. Chem. C*, 2017, **5**, 8355–8360.

45 J. Feng, X. Yan, Y. Liu, H. Gao, Y. Wu, B. Su and L. Jiang, *Adv. Mater.*, 2017, **29**, 1605993.

46 A. Waleed, M. M. Tavakoli, L. Gu, S. Hussain, D. Zhang, S. Poddar, Z. Wang, R. Zhang and Z. Fan, *Nano Lett.*, 2017, **17**, 4951–4957.

47 X. Li, D. Yu, J. Chen, Y. Wang, F. Cao, Y. Wei, Y. Wu, L. Wang, Y. Zhu, Z. Sun, J. Ji, Y. Shen, H. Sun and H. Zeng, *ACS Nano*, 2017, **11**, 2015–2023.

48 X. Liu, D. Yu, F. Cao, X. Li, J. Ji, J. Chen, X. Song and H. Zeng, *Small*, , DOI:10.1002/smll.201700364.

49 M. I. Saidaminov, M. A. Haque, J. Almutlaq, S. Sarmah, X. H. Miao, R. Begum,

Published on 08 January 2019. Downloaded by Queen Mary, University of London on 1/13/2019 5:07:49 PM.

Nanoscale Accepted Manuscript

View Article Online
DOI: 10.1039/C8NR08890J

A. A. Zhumekenov, I. Dursun, N. Cho, B. Murali, O. F. Mohammed, T. Wu and O. M. Bakr, *Adv. Opt. Mater.*, , DOI:10.1002/adom.201600704.

50 J. Song, Q. Cui, J. Li, J. Xu, Y. Wang, L. Xu, J. Xue, Y. Dong, T. Tian, H. Sun and H. Zeng, *Adv. Opt. Mater.*, , DOI:10.1002/adom.201700157.

51 M. Shoaib, X. Wang, X. Zhang, X. Wang, H. Zhou, T. Xu, X. Hu, H. Liu, X. Fan, W. Zheng, T. Yang, S. Yang, Q. Zhang, X. Zhu, L. Sun and A. Pan, *J. Am. Chem. Soc.*, 2017, **139**, 15592–15595.

52 T. Yang, Y. Zheng, Z. Du, W. Liu, Z. Yang, F. Gao, L. Wang, K. C. Chou, X. Hou and W. Yang, *ACS Nano*, 2018, **12**, 1611–1617.

53 M. Kulbak, D. Cahen and G. Hodes, *J. Phys. Chem. Lett.*, 2015, **6**, 2452–2456.

54 D. J. As, F. Schmilgus, C. Wang, B. Schöttker, D. Schikora and K. Lischka, *Appl. Phys. Lett.*, 1997, **70**, 1311–1313.

55 X. Zhao, T. Liu, Y. Cui, X. Hou, Z. Liu, X. Dai, J. Kong, W. Shi and T. J. S. Dennis, *Nanoscale*, 2018, **10**, 8170–8179.

56 X. Zhao, T. Liu, W. Shi, X. Hou, Z. Liu and T. J. S. Dennis, *J. Phys. Chem. C*, 2018, **122**, 8822–8828.

57 X. Zhao, T. Liu, H. Liu, S. Wang, X. Li, Y. Zhang, X. Hou, Z. Liu, W. Shi and T. J. S. Dennis, *ACS Appl. Mater. Interfaces*, 2018, **10**, 42715–42722.

Published on 08 January 2019. Downloaded by Queen Mary, University of London on 1/13/2019 5:07:49 PM.

Nanoscale Accepted Manuscript

TOC

View Article Online
DOI: 10.1039/C8NR08890J

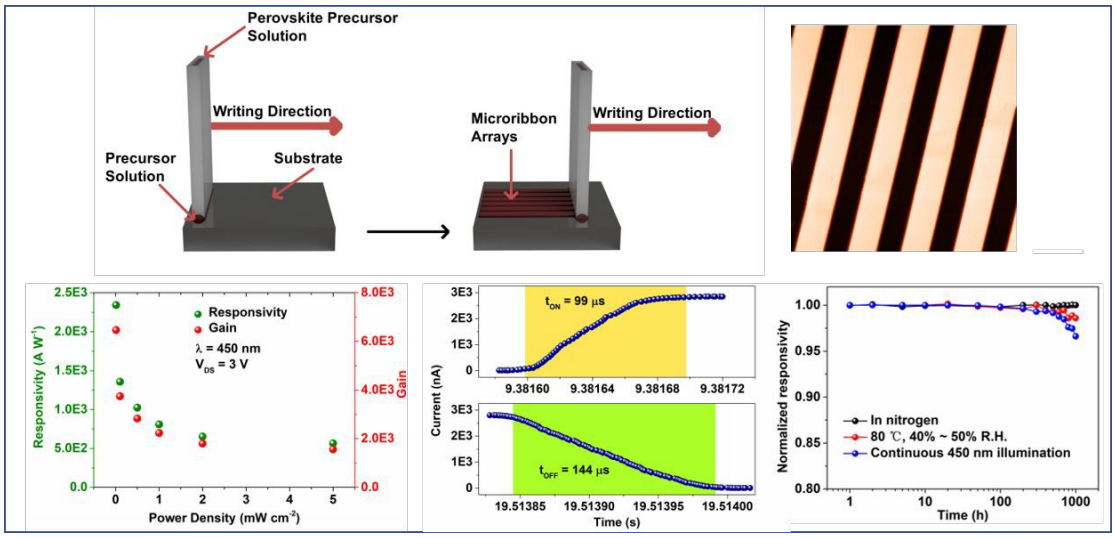

Published on 08 January 2019. Downloaded by Queen Mary, University of London on 1/13/2019 5:07:49 PM.

Nanoscale Accepted Manuscript